Journal of Environmental Management 349 (2024) 119452

Contents lists available at ScienceDirect

Journal of Environmental Management

journal homepage: www.elsevier.com/locate/jenvman

Research article

Equilibrium, transient dynamics and sustainable reference points under age-specific natural mortality rates and varying levels of population productivity: The case of the Northern cod stock

Diana González-Troncoso [a,1], José M. Maroto [b,c,*,1], M. Eugenia Mera [d,1], Manuel Morán [c,d,1]

[a] Instituto Español de Oceanografía (IEO-CSIC), Subida a Radio Faro, 50, 36390, Vigo, Spain
[b] Department of Economía Financiera y Actuarial y Estadística, Universidad Complutense, 28223, Madrid, Spain
[c] IMI-Institute of Interdisciplinary Mathematics, Universidad Complutense, 28040, Madrid, Spain
[d] Department of Análisis Económico y Economía Cuantitativa, Universidad Complutense, 28223, Madrid, Spain

ARTICLE INFO

Handling Editor: Jason Michael Evans

Keywords:
Age-specific natural mortality
Age-structured models
Equilibrium
Fisheries management and conservation
Marine fisheries
Northern cod stock collapse
Transient dynamics

ABSTRACT

Scientific advisory bodies provide scientific advice for sustainable fisheries management based on the precautionary approach and maximum sustainable yield (MSY) reference points, such as spawning stock biomass (SSB) value B_{lim}, and fishing mortality giving MSY, F_{MSY}. The lack of a stock-recruitment function (SRF) to identify a clear breakpoint B_{lim} has recently emerged in important stock collapses. It also precludes the use of equilibrium-based methods to analyze the sustainability of F_{MSY}. Considering a hockey stick (HS) SRF, we propose here an equilibrium-based method that characterizes the equilibriums, their stability properties, transient dynamics, and changes in productivity (including age-specific natural mortality rates). We show that these relevant factors, not taken into account in standard methods, should play a central role in fisheries management and conservation. Considering the Northern cod stock (NCS) (*Gadus morhua*) by way of illustration, we properly estimate the HS and its associated B_{lim}. We find that the HS fitted by the Fisheries Library in R underestimates B_{lim}. Additionally, we determine the levels of productivity (medium-low or medium-high), and their corresponding growth rates of the SSB, which are consistent with the observed population dynamics. We find that the NCS was managed during the 1980s under myopic (unsustainable) harvest control rules, neglecting high age-specific natural mortality rates. We also find that recovery of the NCS remains a distant prospect, despite the current stable, positive equilibrium (sustainable F_{MSY}).

1. Introduction

Equilibrium-based methods are widely used in literature on fisheries management to analyze the sustainability of the main reference points. A crucial stage in these methods consists of properly estimating the stock–recruitment function (SRF) to clearly identify the breakpoint B_{lim}, which is defined by The International Council for the Exploration of the Sea (ICES) as the spawning stock biomass (SSB) value, below which a stock is considered to have reduced reproductive capacity. ICES (2021) provides a framework for estimating B_{lim} using a wide range of SSB-recruitment data (x-R scatter plots) grouped by type and specific stock information. B_{lim} is frequently derived from an analysis of these x-R scatter plots by fitting SRF, such as the widely used Beverton-Holt and hockey-stick (HS) (Froese et al., 2016; ICES, 2021). ICES (2021) also provides guidelines for best practices in the selection of SRF depending on x-R scatter plots.

The fishing mortality giving maximum sustainable yield (MSY), F_{MSY}, is also a key reference point for sustainable fisheries management, such that fishing mortality should be less than F_{MSY} (Mesnil and Rochet, 2010). ICES (2021) also provides guidelines for best practices in the selection of SRF used to estimate F_{MSY}.

The Fisheries Library in R (FLR) (Kell et al., 2007) is a useful toolbox widely used in fisheries management to estimate SRF, B_{lim}, and F_{MSY} (ICES, 2011; Froese et al., 2016). FLR provides precise estimates of B_{lim} in the case of the HS, which is frequently assumed when data do not support more elaborate functions (Cadigan, 2006; Mesnil and Rochet,

* Corresponding author. Department of Economía Financiera y Actuarial y Estadística, Universidad Complutense, 28223, Madrid, Spain.
E-mail addresses: diana.gonzalez@ieo.csic.es (D. González-Troncoso), maroto@ccee.ucm.es (J.M. Maroto), mera@ccee.ucm.es (M.E. Mera), mmoranca@ccee.ucm.es (M. Morán).

[1] These authors contributed equally to this work, and they are listed in alphabetical order.

https://doi.org/10.1016/j.jenvman.2023.119452
Received 24 June 2023; Received in revised form 12 October 2023; Accepted 21 October 2023
Available online 6 November 2023
0301-4797/

2010; ICES, 2011; Froese et al., 2016).

Thus, the ICES framework and FLR provide theoretically and empirically-grounded methods for the estimation of SRF, B_{lim}, and F_{MSY}, with a wide range of applications for most fish stocks. However, these methods could not guarantee a proper estimation of SRF and key reference points for depleted, or previously depleted and recovering fish stocks, where the high variability commonly observed in the x-R data may be exacerbated by the lack of data on intermediate spawning stock size. In these cases, the x-R scatter plots do not conform to the types established by ICES.

The above x-R scatter plot was observed for the Northern cod stock (NCS) (NAFO Divisions 2J3KL) by Fisheries and Oceans Canada (DFO) (DFO, 2019a). NCS is the most iconic case of an unrecovered fishery, once one of the world's largest commercial fisheries which collapsed in the early 1990s (Fig. 1) and remaining in the critical zone of the DFO's Precautionary Approach framework (DFO, 2019b; NAFO, 2021).

Considering the NCS, the first aim of this paper is to properly estimate the SRF and its associated B_{lim}, based on the standard criterion of the goodness of fit to the data. Using non-linear regression methods (NLS), we show that a HS with B_{lim} located in the region at high SSB levels is the model of best fit. We also show that FLR underestimates B_{lim}.

Once the SRF has been estimated, simulation-based approaches (SBA) are widely used in fisheries management to analyze the sustainability of key reference points, such as F_{MSY}, by projecting an age-structured model to equilibrium under different fishing mortality rates and a constant natural mortality rate M (typically M=0.2) (Duplisea, 2012; ICES, 2014). Using a HS, and assuming constant M, these SBA have also been used to analyze the sustainability of F_{MSY} under varying levels of population productivity (Morgan et al., 2014a, 2014b). These SBA fail to account for age-specific natural mortality rates, the characterization of the equilibriums and their stability properties.

In the aforementioned SBA, the sustainability of F_{MSY} is only based on the existence or nonexistence of a positive SSB equilibrium (Morgan et al., 2014a, 2014b). This approach fails to account for transient dynamics (dynamics toward equilibrium) which characterize the behavior of a dynamic system before long-term equilibrium is achieved.

Understanding transient dynamics remains one of the challenges in fisheries management (Maroto and Morán, 2019, and references therein). Transient dynamics analysis, in contrast to SBA, considers not only the existence or nonexistence of a positive SSB equilibrium, but also the growth rate of the SSB and the time required to achieve it.

In this paper we develop an equilibrium-based method that characterizes the equilibriums, their stability properties, transient dynamics and changes in productivity in age-structured models. This age-specific mortality model (ASMM) allows us to determine a sufficient condition for the stability of the positive equilibrium which depends on the main components of population productivity, including age-specific natural mortality rates. Considering the NCS, the main contributions of this paper are to show the following. First, we show that the ASMM allows us to test whether different HS, and their associated B_{lim}, of best fit using different regression methods, as noted above, are also consistent with the observed population dynamics. We show that the HS of best fit to the data estimated by NLS, as noted above, is also consistent with the observed population dynamics. We also show that the HS estimated by FLR is not consistent with the observed population dynamics, dramatically underestimating B_{lim}. Secondly, using a rigorous robustness requirement, we show that the ASMM allows for robust short-term forecasting to determine the levels of productivity (medium-low or medium-high), and corresponding SSB growth rates (low or high) consistent with the observed population dynamics for different short-term periods considered. The sustainability of F_{MSY} for these periods is also analyzed. Thirdly, we find that such periods were characterized by scenarios of collapse not contemplated in existing methods; that is, scenarios of potential collapse, and collapse of the stock with very slow recovery, despite the existence of a stable positive SSB equilibrium and low fishing mortality. Lastly, we analyze the implications of such scenarios for fisheries management and conservation. We find that the NCS was managed during the 1980s under myopic (unsustainable) harvest control rules, neglecting high age-specific natural mortality rates. We also find that recovery of the NCS remains a distant prospect, despite the existence of a stable positive equilibrium (sustainable F_{MSY}). In this regard, we show that transient dynamics are crucial in understanding the observed collapse and slow recovery of many fish stocks which are far from their long-term positive equilibriums. The duration of the transient period is expected to increase in collapsed fisheries which could take a long time to recover under high age-specific natural mortality rates, even when fishing mortality has been reduced.

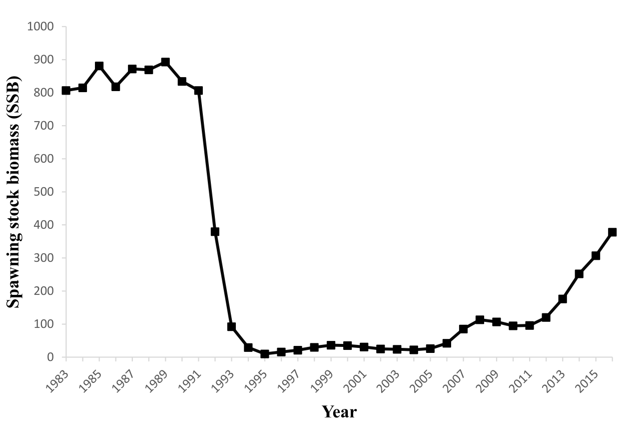

Fig. 1. SSB (1000 tons) for the NCS for the period 1983–2016 from DFO (2018).

2. Material and methods

2.1. Stock-recruitment function (SRF)

Using estimates of SSB-recruitment data from DFO (2018), NLS and FLR, which uses the maximum likelihood method, are used to estimate different SRF for the NCS for the period (1983–2018). The curve fitting toolbox of Matlab is used in the case of NLS, while FLR is an open-source platform for quantitative fisheries science based on the R statistical language.

The HS SRF is given by

$$f(x) = \begin{cases} C \text{ if } \ x \geq x_{\min} \\ \dfrac{C}{x_{\min}} x \text{ if } \ x < x_{\min}, \end{cases} \tag{1}$$

where $f(x)$ is recruitment, and x is SSB. The HS is a piecewise linear function with $\frac{C}{x_{\min}}$ slope at the origin, and constant recruitment C above a breakpoint $x_{\min}$ of SSB which is the precautionary approach reference point B_{lim}, as defined above.

2.2. Age-structured model with constant age-specific mortality rates

The population is divided into n-m+1 age groups (cohorts), where $x_i(k)$ denotes the population numbers of age i at time k, $i=m, \ldots, n$, $k=0,1,2, \ldots$ In each period k, there is a unique mature cohort (n-plus age group) $x_n(k)$ which gives rise to the population of age m (minimum age of recruitment) in period $k+1$, $x_m(k+1)$, through a nonlinear SRF f, such that $x_m(k+1) = f(x_n(k)w_n)$, where $x_n(k)w_n$ is the SSB, and w_n the mean-weighted weight, measured in Kg, at age n. Assuming constant survival rates (time-independent) β_i for each cohort, the deterministic age-structured model is the nonlinear and autonomous dynamic system

$$
\begin{aligned}
x_m(k+1) &= f(x_n(k)w_n) \\
x_i(k+1) &= \beta_{i-1}x_{i-1}(k), i = m+1, \ldots, n-1 \\
x_n(k+1) &= \beta_{n-1}x_{n-1}(k) + \beta_n x_n(k).
\end{aligned} \tag{2}
$$

In the case of NCS, the model has four age groups with the SSB at age n=5+ (a plus 5–14 group), which gives rise to recruitment at age m=2 through a HS SRF f, as defined in (1).

2.3. Sufficient condition for the stability of the equilibrium and changes in productivity

Denoting the mature population in equilibrium by x_n^e, as measured in population numbers, the equilibrium conditions are given by

$$
\begin{aligned}
x_m^e &= f(x_n^e w_n) \\
x_i^e &= \beta_{i-1}x_{i-1}^e, i = m+1, \ldots, n-1 \\
x_n^e &= \beta_{n-1}x_{n-1}^e + \beta_n x_n^e.
\end{aligned} \tag{3}
$$

Inserting the first equation of system (3) into the second equation, $x_{m+1}^e = \beta_m f(x_n^e w_n)$, system (3) can be solved recursively as follows

$$
\begin{aligned}
x_i^e &= \beta_{i-1}\beta_{i-2}\ldots\beta_m f(x_n^e w_n), i = m+1, \ldots, n-1 \\
x_n^e &= \beta_{n-1}\beta_{n-2}\ldots\beta_m f(x_n^e w_n) + \beta_n x_n^e.
\end{aligned} \tag{4}
$$

The SSB in equilibrium $x_n^e w_n$, from which the equilibria of all other cohorts can easily be obtained, can now be derived by rewriting the last equation of system (4)

$$
\begin{aligned}
x_n^e w_n &= \frac{1}{\beta^*} f(x_n^e w_n) w_n, \\
\text{where} \quad \beta^* &= \frac{1-\beta_n}{\beta_{n-1}\beta_{n-2}\ldots\beta_m}.
\end{aligned} \tag{5}
$$

Using (3), (5), and the theory of non-linear dynamic systems, a sufficient condition for the stability of the equilibrium is determined in Maroto and Morán (2019).

$$
f'(x_n^e w_n) < \frac{\beta^*}{w_n} = \frac{f(x_n^e w_n)}{x_n^e w_n}. \tag{6}
$$

In the case of the HS, as defined in (1), the condition for the stability of the equilibrium, as defined in (6), is met if $x_n^e w_n > x_{\min}$ due to the fact that $f'(x_n^e w_n) = 0 < \frac{f(x_n^e w_n)}{x_n^e w_n}$.

Thus, the condition for the stability of the positive equilibrium (CSPE) in the case of the HS is given by $x_n^e w_n > x_{\min}$ which, using (5), can be rewritten as

$$
\frac{C}{x_{\min}} > \frac{\beta^*}{w_n}. \tag{7}
$$

If the CSPE, as defined in (7), is met, then, using (5), there is a unique asymptotically stable positive SSB equilibrium $x_n^e w_n = \frac{C w_n}{\beta^*} > x_{\min}$ (Maroto and Morán, 2019) (hereafter $x_n^e w_n = \overline{x}$). This means that if the CSPE is met the positive SSB equilibrium $\overline{x} > x_{\min}$ is determined by the intersection of the linear function (replacement line) $g(x) = \frac{\beta^*}{w_n} x$ and the HS, where the slope of $g(x)$, $\frac{\beta^*}{w_n}$, is lower than the slope of the HS $\frac{C}{x_{\min}}$ and, consequently, $g(x)$ intersects the HS to the right of the SSB breakpoint $x_{\min}$ (positive SSB equilibrium $\overline{x} > x_{\min}$).

The CSPE, as defined in (7), depends on recruits per spawner (RPS), one of the key metrics of productivity (Morgan, 2019), as measured by the slope of the HS $\frac{C}{x_{\min}}$. It also depends on other key metrics of productivity, as the composite cohort survival rate $\beta^* = \frac{1-\beta_n}{\beta_{n-1}\beta_{n-2}\cdots\beta_m}$, contemplating age-specific fishing F_i and age-specific natural mortality M_i rates through the survival rate at age i, $\beta_i = e^{-(F_i+M_i)}$, and weight-at-age through w_n, as defined in (2).

In the case of the HS, variations in population productivity can be measured by variations in RPS (slope $\frac{C}{x_{\min}}$ of the HS), maintaining constant the SSB breakpoint $x_{\min}$, where it is assumed that $x_{\min} = B_{\lim}$ does not vary with productivity (Morgan et al., 2014a, 2014b). Thus, the CSPE allows us to analyze changes in productivity for different periods, as measured by changes in RPS (changes in $\frac{C}{x_{\min}}$), taking also into account other main components of productivity (hereafter $x_{\min}$ and $B_{\lim}$ will be used indistinctly, as $x_{\min} = B_{\lim}$).

In Cadigan (2016), a state-space integrated assessment model (NCAM) is developed to estimate age-specific natural mortality rates for the NCS. NCAM is the official assessment model used by DFO (Brattey et al., 2018; DFO, 2018). Estimates of F_i and M_i (i=2, 3, and 4) are obtained from Brattey et al. (2018), and of the mean F_n and the mean M_n, at age n=5+ (a plus 5–14 group), from DFO (2018). These age-specific data allow us to obtain estimates of the mean M-at-age, and the mean F-at-age and, therefore, to obtain estimates of the mean cohort survival rate β-at-age and, consequently, of β^*, as defined in (5), for each period considered. The SSB mean-weighted weight w_n (age n=5+) is obtained for each period of k years, using estimates of the mean weight-at-age for that period, the abundance-at-age at the end of the k-year period, and the total abundance at the end of the k-year period from Brattey et al. (2018).

Using the above estimates, a standard spreadsheet software (e.g. Excel) can be used in order to test if the CSPE is met for each period considered.

2.4. Sustainability of fishing mortality reference points

The CSPE allows us to analyze changes in productivity for different periods, as measured by changes in $\frac{C}{x_{\min}}$, keeping constant $x_{\min}$, as noted above. For each period considered, and its corresponding value of $\frac{C}{x_{\min}}$, the SSB x_{MSY} and the fishing mortality F_{MSY} can be determined using the package Reference Points for Fisheries Management (FLBRP) of FLR. Data used in FLR to estimate x_{MSY} and F_{MSY} are obtained from Brattey et al. (2018): landings, catch-at-age, mean weight at age in the catch, mean weight at age in the stock, natural mortality at age, maturity at age, stock numbers at age, and fishing mortality at age.

For each period considered, and its corresponding value of $\frac{C}{x_{\min}}$, F_{MSY} is sustainable if the CSPE is met for the fishing mortality rate of the SSB F_n=F_{MSY} (for the survival rate of the SSB $\beta_n = e^{-(F_{MSY}+M_n)}$), and for M_n, $\beta_{n-1}\beta_{n-2}\ldots\beta_m$, and w_n estimated for such a period. In this case, the SSB x_{MSY} is an asymptotically stable positive equilibrium $\overline{x} = x_{MSY} > B_{\lim}$. This means that the replacement line g(x), where F_n=F_{MSY} in β*, intersects the HS to the right of $B_{\lim}$. Sustainable fishing at levels below F_{MSY}, $F_n < F_{\text{MSY}}$, will result in a positive SSB equilibrium that is greater than x_{MSY}, $\overline{x} = \frac{C w_n}{\beta^*} > x_{MSY} > B_{\lim}$ and, consequently, F_{MSY} is sustainable.

By contrast, if the CSPE is not met for F_n=F_{MSY}, then F_{MSY} is not sustainable. In this case, the replacement line $g(x)$ does not intersect the HS to the right of $B_{\lim}$ (absence of positive SSB equilibrium), with the consequent population decline and eventually collapse of the species. In this case, F_{MSY} is zero, and no level of fishing mortality F_n is sustainable.

The CSPE can be rewritten in terms of F_{crash}, fishing mortality corresponding to the slope $\frac{C}{x_{\min}}$ of the HS (Mesnil and Rochet, 2010; ICES, 2011)

$$
\beta^* = \frac{1 - e^{-(M_n+F_{crash})}}{\beta_{n-1}\beta_{n-2}\ldots\beta_m} = \frac{C w_n}{x_{\min}}. \tag{8}
$$

Without loss of generality, F_{crash}, as derived from Eq. (8), represents the fishing mortality rate of the SSB F_n for which the SSB equilibrium $\overline{x} = x_{\min} = B_{\lim}$ is achieved, taking into account that the very low fishing mortality rates of all other cohorts F_i, as estimated in Brattey et al. (2018), are included in the denominator of Eq. (8), $\beta_i = e^{-(F_i+M_i)}$, i=m, …,n-1.

Based on the above, if F_{MSY} is sustainable, then $F_{\text{MSY}} < F_{crash}$.

2.5. Transient dynamics

Assuming constant survival rates β_i, as defined in (2), Eq. (9) below, describes well the population dynamics of the SSB which is autonomous (dependent on itself), but with a delay of n-m+1 reproductive periods

$$x_n(k+1)w_n = \beta_{n-1}\beta_{n-2}...\beta_m f(x_n(k+m-n)w_n)w_n + \beta_n x_n(k)w_n. \quad (9)$$

If the SRF f is the HS, Eq. (9) is a piecewise linear dynamic that can be used to analyze transient dynamics. In particular, if the CSPE is met, the SSB converges to the stable positive SSB equilibrium $\overline{x} = \frac{Cw_n}{\beta^*} > x_{\min}$ at an exponential rate λ_n^k (Maroto and Morán, 2019). Using Eq. (9) for the NCS, the value of λ_n can be obtained: *i)* if the SSB level x is lower than $x_{\min}$, $x < x_{\min}$, then $f(x) = \frac{C}{x_{\min}}x$ and $\lambda_n = \lambda_{\max}$, where $\lambda_{\max} > 1$ is the largest real root of the characteristic polynomial $P_1(\lambda) = \lambda^4 - \beta_n\lambda^3 - \beta_4\beta_3\beta_2\frac{Cw_n}{x_{\min}}$, and x grows exponentially, and *ii)* if $x \geq x_{\min}$, then $f(x) = C$, and the distance between x and $x_{\min}$ tends to zero exponentially with $\lambda_n = \beta_n$, where β_n<1 (survival rate of the SSB) coincides with the unique positive root of the characteristic polynomial $P_2(\lambda) = \lambda^4 - \beta_n\lambda^3$.

It should be noted that $P_1(\lambda)$ and $P_2(\lambda)$ are the characteristic polynomials of the linearization of Eq. (9) around the unstable $\overline{x}= 0$, and the asymptotically stable $\overline{x} = \frac{Cw_n}{\beta^*} > x_{\min}$, SSB equilibriums, respectively.

The characteristic polynomials $P_1(\lambda)$ and $P_2(\lambda)$ can be solved using mathematical software (e.g. Maplesoft Maple) in order to find the value of λ_n for each period considered. In this way, the predicted growth of the SSB by the model during a period of k years is given by

$$x_k = \begin{cases} \overline{x} + (x_{k_0} - \overline{x})\lambda_n^k \text{ if } x_{k_0} \geq x_{\min} (case\ ii) \\ x_{k_0}\lambda_n^k \text{ if } x_{k_0} < x_{\min} (case\ i) \end{cases} \quad (10)$$

where x_k is the SSB level achieved at the end of the k-year period, if x_{k_0} is the SSB level at the start of the period.

Using Eq. (10), the growth of the SSB can be simulated from the beginning of the period considered, predicting the SSB level achieved at the end of the k-year period. In order to do this, the confidence interval estimated by DFO (2018) for the SSB level at the start of the period (Table 1) is partitioned into fifty equally spaced initial SSB levels x_{k_0}, as defined in Eq. (10). For each x_{k_0}, the SSB level achieved at the end of the k-year period, x_k, is obtained using Eq. (10). Then, for each x_{k_0}, we test whether its corresponding x_k falls within the confidence interval estimated by DFO (2018) for the SSB level observed at the end of the k-year period. This is a rigorous robustness requirement that autonomous models must meet in order to describe the observed growth of the species by obtaining robust forecasting, at least for short-term periods.

Using Eq. (10), and the confidence intervals estimated by the DFO (2018) for the periods considered (Table 1), the above robustness requirement can be carried out using a standard spreadsheet software (e.g. Excel).

Table 1
SSB (1000 tons) for different years (k).

Year (k)	x_k	$[x_{kL}, x_{kU}]_{DFO}$
1983	807	[673,968]
1990	834	[646,1077]
2004	22	[18,26]
2011	96	[79,117]
2014	252	[211,301]
2015	307	[257,367]
2016	378	[312,457]
2017	441	[350,556]
2021	411	[307,549]

Notes: $[x_{kL}, x_{kU}]_{DFO}$ is the 95% confidence interval estimated by DFO (2018), and NAFO (2021) (row 10), for the SSB level x_k.

3. Results

3.1. Estimation of the stock-recruitment function (SRF)

The SSB-recruitment (x-R) scatter plot for the NCS for the period 1983–2018 (Fig. 2) reflects the lack of x-R data on intermediate SSB levels, where most x-R data are concentrated at low SSB levels. This x-R scatter plot is divided into two clearly delimited regions, at low and high SSB levels, which correspond to the periods 1992–2018, where the stock collapsed (Fig. 1), and 1983–1991, respectively.

Using NLS, and the functions *bevholt* and *segreg* of FLR, which are based on the maximum likelihood method, the widely used Beverton-Holt (BH) and HS SRF were fitted to the x-R data of NCS (Fig. 2 and Table 2).

In the case of NLS, the BH and the HS show similar fits to the x-R data (similar values of the mean squared error (MSE) and R^2) (columns 5 and 6) by reflecting a linear relationship between SSB and recruitment. In this case, the MSE and R^2 values are similar than those obtained in the case of linear least squares regression (LS) (row 2). It can be shown that this result is also obtained by fitting other SRF, as the smoothing version of the HS (bent hyperbola) developed in Mesnil and Rochet (2010). In the case of the HS, this linear relationship is obtained both with and without fixing $x_{\min}$ (rows 3–5). In all of these cases, this linear relationship implies that the SSB breakpoint of best fit, $x_{\min}$=881 (row 5) (lower MSE value and higher R^2 value), is located in the region at high SSB levels $x_{\min} \in [881,893]$, where $x_{\min}$=893 (row 4 and Fig. 2) is the highest observed SSB.

It should be noted that, in the case of NLS, our own algorithm has also been developed to fit the HS using the L1-norm regression (least absolute deviations), with similar results to those obtained using the L2-norm (least squares deviations). This confirms the robustness of the HS fitted by NLS.

Estimates from FLR are quite different from those obtained in the case of NLS (rows 4–6 and Fig. 2). In the case of the HS with $x_{\min}$ as a free parameter (row 5 and Fig. 2), the SSB breakpoint of best fit is located in the region at low SSB levels $x_{\min}$ =153.4 which is distant from those obtained by NLS $x_{\min} \in [881,893]$ (Fig. 2 for the case of $x_{\min}$ =893). This result is also obtained by using the Julious Algorithm (Julious, 2001) which overcomes issues associated with local minima. In the case of the BH estimated by FLR, which is the model of best fit (lower Akaike information criterion (AIC) value), the asymptote to the relationship is also located at low SSB levels, $x_A = a/b$=557 (row 6 and Fig. 2). Consequently, this case is also distant from the linear relationship estimated by NLS in the case of the BH (estimated parameter b=0 in row 6). Additionally, in contrast to NLS, FLR provides different fits to the x-R data, if the BH and the HS are fitted (rows 4–6 and Fig. 2).

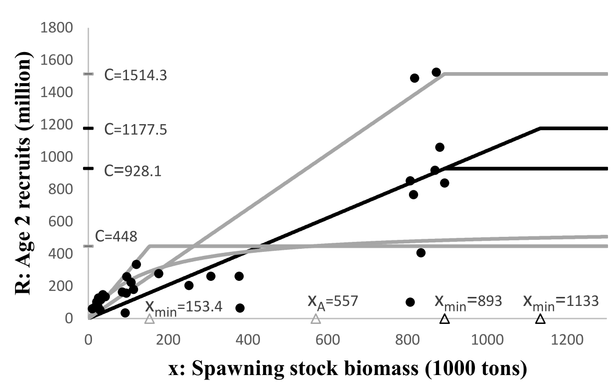

Fig. 2. x-R estimates for the NCS for the period 1983–2018 from DFO (2018). Best fit to BH and HS SRF using FLR (light lines at low x values). HS, with $x_{\min}$=893, estimated by FLR (light line at high x values). HS, with $x_{\min}$=893 and $x_{\min}$=1133, using NLS (dark lines).

Table 2
Estimated parameters of different stock-recruitment functions (models) using different regression methods and FLR.

Model	Method	Parameter	Estimate	MSE	R^2	AIC
Linear: $f(x) = ax$	LS	a	1.039	56157.657	0.64467	
HS: $x_{min} = 1133$	NLS	C	1177.5	56157.657	0.64467	
HS: $x_{min} = 893$	NLS	C	928.1	56157.657	0.64505	
	FLR	C	1514.3			16.4
HS: x_{min} = free	NLS	C	917.2	56096.993	0.64505	
		$x_{\min}$	881			
	FLR	C	448			4.7
		$x_{\min}$	153.4			
BH: $f(x) = \frac{ax}{1+bx}$	NLS	$a \geq 0$	1.04	56157.659	0.64467	
		$b \geq 0$	0			
	FLR	$a \geq 0$	3.9			−2.9
		$b \geq 0$	0.007			

Thus, the above results show that different regression methods provide quite different estimates of $x_{\min}$, even for the same fitted SRF. The reason for this is that FLR assumes lognormal error, which implies that estimates of $x_{\min}$ and C are much lower than those estimated by NLS which assumes normal error. It also explains that, in contrast to NLS, if $x_{\min}$ is fixed at high SSB levels of the HS, worse fits to the x-R data are obtained by FLR (higher AIC values) (row 4, column 7, and Fig. 2). Thus, in contrast to NLS, FLR is not able to detect a linear relationship between SSB and recruitment.

In the case of the NCS, DFO (2019a) suggests a linear relationship between SSB and recruitment. According to this linear relationship, a HS with $x_{\min} \in [881,893]$ fitted by NLS is the model of best fit to data for the NCS. This is also consistent with the suggestion of DFO (2019a) that $x_{\min}$ should be at the highest observed SSB $x_{\min}$=893 (row 4 and Fig. 2), where the underlying hypothesis is that the SSB was always below $x_{\min}$ during the whole period considered 1983–2018. However, this hypothesis, which plays an important role in transient dynamics analysis, as defined in Eqs. (9) and (10), is not met even in the case of $x_{\min} = 893$. The reason for this is that, as described below, there exists the probability of exceeding $x_{\min} = 893$ when simulating the growth of the SSB. In order to guarantee that this hypothesis will be met, the upper bound of the confidence interval estimated by DFO for the highest SSB, [704, 1133], could be considered as $x_{\min}$ =1133. Additionally, this case shows the same best fit to the x-R data (same values of MSE and R^2) than that obtained in the case of $x_{\min}$=893 (rows 3 and 4, columns 5 and 6, and Fig. 2). The reason for this is that for SSB values greater than the highest observed SSB, $x_{\min}$ >893, where there is a lack of x-R data, the estimated parameter C in fitting the HS preserves the slope of the HS estimated for the case of $x_{\min} = 893$ (Fig. 2).

Thus, considering the hypothesis suggested by DFO (2019a), a HS with $x_{\min} = B_{\lim}$=1133 fitted by NLS is the model of best fit to the x-R data for the NCS (row 3, and Fig. 2). The case where this hypothesis is not met, $x_{\min} \in [893, 1133]$, will also be analyzed in this paper.

3.2. Equilibrium, transient dynamics, changes in productivity, and sustainability of F_{MSY}

The CSPE, as defined in (7), and transient dynamics, as defined in Eqs. (9) and (10), are analyzed for different relevant short-term periods inside the whole period observed 1983–2018, where constant survival rates β_i, as defined in (2), is a reasonable assumption.

3.2.1. Pre-collapse period (1983–1990)

This period was characterized by slow growth, where the SSB estimated by DFO for the year 1990, x=834, is close to that estimated for the year 1983, x=807 (Fig. 1 and Table 1).

Using estimates of β^*=1.32 and w_n=1.56 (age n = 5+) for this period, the CSPE is met for values of the slope of the HS $\frac{C}{x_{\min}} \geq \frac{\beta^*}{w_n} = 0.85$, or in terms of recruitment for values of $C \geq \frac{\beta^* x_{\min}}{w_n} = 959$ (Table 3, column 2, rows 7–10). This implies that the CSPE was met during this period for the HS of best fit to the x-R data estimated by NLS, with $B_{\lim}$=1133 and estimated parameter C=1177.5 (Table 2, row 3). However, it can be shown that, for C=1177.5, thirty-four percent of the times the SSB predicted by the model for the year 1990 is greater than $B_{\lim}$=1133. Consequently, as noted above, the initial hypothesis that the SSB was always below $B_{\lim}$ is not met.

Levels of productivity $\frac{C}{x_{\min}} \in [0.85,0.96]$ ($C \in [968,1086]$) guarantee both that the CSPE to be met and that the SSB was always below $B_{\lim}$=1133 of best fit. In this regard, transient dynamics analysis is carried out for these levels of productivity (Table 4), where the HS f, as defined in (9), is given by $f(x) = \frac{C}{x_{\min}}x$. Using Eq. (10) (case *i)*), the model fits well with the slow growth of the SSB observed during the pre-collapse period (1983–1990) for these levels of productivity (Table 4).

For values of $\frac{C}{x_{\min}} \in [0.85,0.92]$ (row 2), and $\frac{C}{x_{\min}} \in (0.92,0.96]$ (rows 3–5), the SSB predicted by the model for the year 1990 always falls (one hundred per cent), and almost always falls, [84%, 100%) (column 4), respectively, within the confidence interval estimated by DFO for that year (Table 1). The reason for this is the low growth exponential rate λ_n^k, where $\lambda_n \in (1,1.022]$ (column 3), which is greater than, but close to 1, which means that the SSB growth is slow, as observed during this period.

Transient dynamics also allow us to analyze the case of the HS with $B_{\lim}$ being the highest observed SSB ($B_{\lim}$=893) (Table 2, row 4) where the hypothesis that the SSB was always below $B_{\lim}$ is not met. Using Eq. (10) (case *i)* and case *ii)*), it can be shown that the model also fits well with the slow growth of the SSB observed during this period for levels of productivity $\frac{C}{x_{\min}} \in [0.86,0.98]$, which are very similar to those obtained in the case of $B_{\lim}$=1133, as analyzed above. In this case, it can be shown that between thirty-six and seventy-six percent of the times the SSB predicted by the model for the year 1990 is greater than $B_{\lim}$=893.

In the case of the HS of best fit estimated by FLR, the SSB was always above $B_{\lim}$=153.4 of best fit (Fig. 1). In this case, the HS f, as defined in (9), is given by $f(x) = C$. Using Eq. (10) (case *ii)*), where $\lambda_n = \beta_n = e^{-(F_n+M_n)} = 0.57$ (Table 3, column 2, row 6), it can be shown that the model does not fits well with the growth of the SSB observed during this period. The reason for this is that the SSB predicted by the model for the year 1990 never falls within the confidence interval estimated by DFO for that year (Table 1). In this case, it can also be shown that the stock would have remained at the end of this period in a neighborhood of the stable positive SSB equilibrium $\bar{x} = \frac{Cw_n}{\beta^*} = 530$, that is well above $B_{\lim}$=153.4. Consequently, the HS estimated by FLR is not consistent with the observed population dynamics for this period.

Thus, the low levels of productivity $\frac{C}{x_{\min}} \in [0.85,0.96]$ (Fig. 3 for the average of these levels) are consistent with the observed low growth of the SSB during the pre-collapse period (1983–1990). This result is consistent with the observed low values of RPS, which were well below the average during this period (Morgan, 2019), in such a way that it is characterized as a period of medium-low productivity. This is consistent with the fact that the late 1980s, which was characterized by low productivity conditions (Morgan, 2019), is considered in the pre-collapse period (1983–1990). This characterization is also consistent with the other main components of low productivity for this period, contemplated in the CSPE and transient dynamics analysis, such as the relatively low w_n=1.56 (Table 3, column 2, row 8), and the high estimated age-specific natural mortality rates M_i (Table 3, column 2), which were greater than those assumed in existing methods (constant M=0.2).

We can observe in Table 4 (columns 5 and 6) that, for the levels of productivity $\frac{C}{x_{\min}} \in [0.85,0.96]$ which are consistent with the observed low growth of the SSB during the pre-collapse period (1983–1990), $F_{MSY} \in [0.2,0.297]$ is very close to $F_{crash} \in [0.204,0.3]$, as defined in (8),

Table 3
The condition for the stability of the positive equilibrium (CSPE) for different periods.

	1983–1990		1991–1994		1991–1994 (R&W)		2004–2011		2011–2014	
Age	*F*	*M*	*F*	*M*	*F*	*M*	*F*	*M*	*F*	*M*
2	0	0.41	0	0.95	0	0.366	0	0.38	0	0.30
3	0.01	0.35	0.01	1.18	0.01	0.366	0	0.35	0	0.25
4	0.04	0.31	0.05	1.21	0.05	0.366	0	0.42	0	0.25
n=5+	0.2	0.36	0.17	2.03	1.23	0.366	0.03	0.46	0.02	0.27
β^*	1.32		26.43		2.53		1.22		0.56	
w_n	1.56		1.025		1.025		1.96		1.79	
$\frac{C}{x_{min}}$	≥0.85		≥25.8		≥2.47		≥0.62		≥0.32	
C	≥959		≥29215		≥2799		≥705		≥358	

Notes: Estimates of age-specific fishing F_i and natural mortality M_i rates are from DFO, and from Rose and Walters (2019) (R&W) (column 4).

Table 4
Transient dynamics analysis for the pre-collapse period (1983–1990).

$\frac{C}{x_{\min}}$	C	λ_n	$x_k \in [x_{kL}, x_{kU}]_{DFO}$	F_{crash}	F_{MSY}
[0.85,0.92]	[968,1047.5]	(1,1.015]	100%	[0.204,0.268]	[0.2,0.266]
(0.92,0.939]	(1047.5,1064]	(1.015,1.018)	[94%,100%)	(0.268,0.282]	(0.266,0.28]
(0.939,0.944]	(1064,1069.6]	[1.018,1.0195]	[90%,94%)	(0.282,0.287]	(0.28,0.284]
(0.944,0.96]	(1069.6,1086]	(1.0195,1.022]	[84%,90%)	(0.287,0.3]	(0.284,0.297]

Notes: The value $x_k \in [x_{kL}, x_{kU}]_{DFO}$ is the percentage of times that the SSB predicted by the model at the end of the *k*-year period, x_k, falls within the confidence interval estimated by DFO for the SSB level observed at the end of the *k*-year period (Table 1).

due to the fact that $x_{MSY} \in [1136,1138]$ is very close to the breakpoint $B_{\lim}$=1133.

For the pre-collapse period (1983–1990), where the CSPE is met, the estimated SSB level in the year 1990, $x = 834$ (Fig. 1), is lower than the SSB equilibrium $\overline{x} > B_{\lim} = 1133$, due to the slow growth of the SSB during this period, as noted above. Using Eq. (10) (case *i)*), with $x_{k_0} = 834$ (Table 1), transient dynamics analysis allows us to determine the growth of the SSB from the year 1990, the equilibrium $\overline{x} = \frac{Cw_n}{\beta^*} > B_{\lim} = 1133$, and the time required to achieve it. In this analysis, the levels of productivity which are consistent with the observed low growth of the SSB during the pre-collapse period (1983–1990), $\frac{C}{x_{\min}} \in [0.85,0.96]$ ($C \in [968,1086]$), are assumed to remain constant since the year 1990. This is

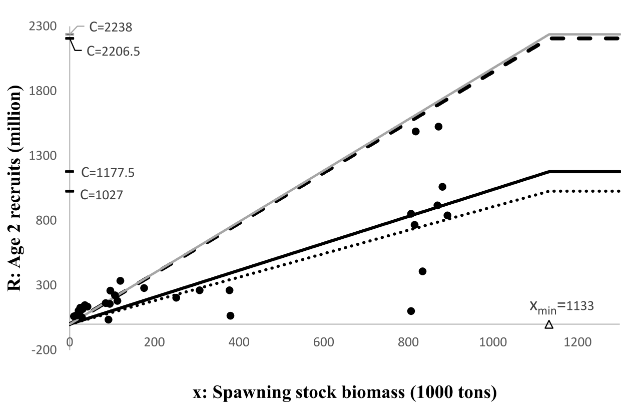

Fig. 3. x-R estimates for the NCS for the period 1983–2018 from DFO (2018). Best fit to HS SRF, with $x_{\min}$=1133 and C=1177.5, using NLS (dark solid line). The average levels of medium-low productivity, $\frac{C}{x_{\min}} = 0.91$ or C=1027, for the pre-collapse period (1983–1990), and for the most recent period (2016–2021) (dotted line). The average levels of medium-high productivity, $\frac{C}{x_{\min}} =$ 1.95 and $\frac{C}{x_{\min}} =$ 1.98, or C=2206.5 and C=2238, for the post-collapse periods (2004–2011) and (2014–2016) (dashed line), and (2011–2014) (light line), respectively.

carried out under different scenarios (different F_n and M_i) (Table 5).

We can observe in Table 5 (rows 2–4) that, if F_n=0.2 (column 3, and Table 3, column 2) and M_i (column 4, and Table 3, column 2) estimated by DFO for the pre-collapse period (1983–1990) had been kept constant since 1990, it would take a long time (column 5) to achieve the SSB equilibrium $\overline{x}$ (column 7) due to the slow growth of the SSB (column 6). Additionally, $\overline{x}$ would be very close to $B_{\lim}$=1133 (column 7). This is also the case for the higher range of productivity levels $\frac{C}{x_{\min}} \in [0.95,0.96]$ (row 5), and for higher values of F_n=0.28, as estimated in Brattey et al. (2018). For lower values of $F_n \in [0.1,0.15]$ (rows 6–11), the required time to achieve a greater SSB equilibrium $\overline{x}$ decreases drastically for all values of $\frac{C}{x_{\min}} \in [0.85,0.96]$ due to the higher growth of the SSB $\lambda_n \in [1.014,1.049]$.

In the case of lower and constant natural mortality rates M =0.2 (row 12), for all values of $\frac{C}{x_{\min}} \in [0.85,0.96]$, and for F_n=0.2, a SSB equilibrium at very high SSB levels $\overline{x} \in [2397,2689]$ well above the $B_{\lim}$=1133, which have never been observed (Fig. 1), is achieved in just four years due to the extremely high growth of the SSB, $\lambda_n \in [1.138,1.163]$. In the case of high F_n=0.44 (row 13), a high SSB equilibrium is achieved in only [5,6] years due to the high growth of the SSB $\lambda_n \in [1.079,1.105]$.

3.2.2. *Collapse period (1991–1994)*

This period was characterized by the dramatic decrease in the SSB, from x=807 in the year 1991 to x=29 in the year 1994 (Fig. 1).

Estimates of F_i from DFO for this period are similar to those estimated for the pre-collapse period (1983–1990), and even lower for F_n (Table 3, columns 2 and 3). However, estimates of M_i are extremely greater than those estimated for the pre-collapse period (1983–1990), increasing more than threefold at age 2–4, and more than sixfold at age n=5+, which gives rise to dramatic decrease in survival rates β_i (increase in β^*) (row 7). Additionally, the estimated value of w_n=1.025 for this period is the lowest w_n in the time series (Table 3, row 8). All of this implies that, for the collapse period (1991–1994), the CSPE is only met for extremely high productivity levels $\frac{C}{x_{\min}} \geq 25.8$ ($C \geq 29215$) (rows 9 and 10), which are not consistent with the observed low values of RPS, which were well below the average during this period (Morgan, 2019). Consequently, F_{MSY} was not sustainable during this period.

Table 5
Transient dynamics analysis from the year 1990.

$\frac{C}{x_{\min}}$	C	F_n	M_{2-4} M_n	t (years)	λ_n	$\bar{x}$
` **[0.85,0.87]**	[968,981.5]	0.2	1.07 0.36	>100	[1.0005,1.0031]	[1145,1161]
[0.88,0.91]	[999,1025]	0.2	1.07 0.36	[30,50]	[1.0064,1.011]	[1181,1212]
(0.91,0.96]	(1025,1086]	0.2	1.07 0.36	[16,30)	(1.011,1.022]	(1212,1284]
[0.95,0.96]	[1079,1086]	0.28	1.07 0.36	>100	[1.0002,1.0015]	[1162,1170]
[0.85,0.87]	[968,981.5]	0.15	1.07 0.36	[21,24]	[1.014, 1.016]	[1231,1249]
[0.88,0.91]	[999,1025]	0.15	1.07 0.36	[14,17]	[1.02,1.025]	[1271,1304]
(0.91,0.96]	(1025,1086]	0.15	1.07 0.36	[10,14)	(1.025,1.035]	(1304,1382]
[0.85,0.87]	[968,981.5]	0.1	1.07 0.36	[12,13]	[1.027,1.03]	[1148,1154]
[0.88,0.91]	[999,1025]	0.1	1.07 0.36	[10,11]	[1.033,1.038]	[1386,1422]
(0.91,0.96]	(1025,1086]	0.1	1.07 0.36	[8,11)	(1.038,1.049]	(1422,1507]
[0.85,0.96]	[968,1086]	0.2	0.6 0.2	4	[1.138,1.163]	[2397,2689]
[0.85,0.96]	[968,1086]	0.44	0.6 0.2	[5,6]	[1.079,1.105]	[1672,1876]

Notes: The value M_{2-4} is the aggregated M_i, i=2, 3, 4 (Table 3, column 2). The value t is the time required to achieve the SSB equilibrium $\bar{x}$. The value λ_n is the growth rate of the SSB.

More reasonable (lower) estimates of M for this period are provided by Rose and Walters (2019), where a virtual population analysis model is used to estimate annual values of M of total biomass, and F_n (n=5+). Without loss of generality, the average $M \approx 1.46$ estimated by Rose and Walters (2019) for the collapse period (1991–1994) is divided equally between the cohorts. These M_i are much lower, but still high, and F_n =1.23 is much higher, than those estimated by DFO, increasing more than sevenfold (Table 3, columns 3 and 4). Using these estimates of M_i and F_n, the CSPE is met for more reasonable (much lower), but still high, productivity levels $\frac{C}{x_{\min}} \geq 2.47$ ($C \geq 2799$), which are not consistent with the observed lowest values of RPS during the collapse period (1991–1994). Consequently, F_{MSY} is still not sustainable, in this case due to high F_n.

Table 6
Transient dynamics analysis for different periods.

Period	$\frac{C}{x_{\min}}$	C	λ_n	$x_k \in [x_{kL}, x_{kU}]_{DFO}$
1983–1990	[0.85,0.96]	[968,1086]	(1,1.022]	[84%,100%]
2004–2011	[1.91,1.99]	[2163,2250]	1.24	100%
2011–2014	[1.94,2.01]	[2196,2280]	1.37	92%
2016–2021	[0.85,0.96]	[968,1086]	(1,1.022]	100%

Notes: The value $x_k \in [x_{kL}, x_{kU}]_{DFO}$ is the percentage of times that the SSB predicted by the model at the end of the k-year period, x_k, falls within the confidence interval estimated by DFO for the SSB level observed at the end of the k-year period (Table 1).

3.2.3. Post-collapse period (2004–2016) and predictive power of the model

The post-collapse period (1995–2016) was characterized by the slow recovery of the SSB (Fig. 1). Four subperiods are differentiated in terms of the growth of the SSB, which was extremely low during the 1995–2004 period where, as showed in Maroto and Morán (2019), it was practically non-existent due to the high M_i, as estimated by DFO. SSB growth increased significantly, with different growth rates, during the 2004–2011, 2011–2014, and 2014–2016 periods (Fig. 1).

Estimates of F_n from DFO for the 2004–2011 and 2011–2014 periods, and of M_i for the 2011–2014 period, are much lower than those estimated for the pre-collapse period (1983–1990) (Table 3, columns 2, 5, and 6), which implies greater survival rates β_i (lower β^*) for those periods (row 7). Additionally, w_n increased significantly during those periods (row 8). All of this implies that, for the post-collapse periods (2004–2011) and (2011–2014), the CSPE is met for values of $\frac{C}{x_{\min}}$ much lower than those required for the pre-collapse period (1983–1990) (row 9).

The model fits well with the high growth of the SSB observed during the post-collapse periods (2004–2011) and (2011–2014) (Table 6, rows 3 and 4). This can be shown using Eq. (10) (case i)) from the confidence interval estimated by DFO for the SSB level at the start of the period (for the year 2004 and year 2011) (Table 1), and for values of $\frac{C}{x_{\min}} \in$ [1.91,1.99], and $\frac{C}{x_{\min}} \in$ [1.94,2.01]. In these cases, the SSB predicted by the model for the year 2011 always falls (one hundred per cent), and for the year 2014 almost always falls, 92 %, respectively, within the confidence interval estimated by DFO for these years (rows 3 and 4, and Table 1). The reason for this is the high growth rates, λ_n =1.24 and λ_n =1.37, respectively (rows 3 and 4, column 4), which are well above 1, which means that the SSB growth is high, as observed during those periods. Using as possible future scenarios these high growth rates, the predictive power of the model can also be evaluated by comparing its stock predictions for the years 2015, 2016, and 2017, if the year 2014 is the start of the period, with those estimated by DFO for those years (Table 7).

The model fits well with the high growth of the SSB observed during the years 2015, 2016, and 2017, if the SSB has grown, from the year 2014, at the rate which is consistent with the observed dynamics during the 2004–2011 (Table 7, rows 2–4). In particular, using Eq. (10) (case i)) for λ_n=1.24, from the confidence interval estimated by DFO for the SSB level at the start of the period (for the year 2014) (Table 1), the SSB

Table 7
Transient dynamics analysis for different periods.

Period	λ_n	$x_k \in [x_{kL}, x_{kU}]_{DFO}$	x_k^*
2014–2015	1.24	100%	
2014–2016	1.24	96%	
2014–2017	1.24	88%	
2014–2015	1.37	62%	
2014–2016	1.37	38%	
2014–2017	1.37	8%	
2016–2021	1.005	100%	$x^*_{2283} \in [1134, 2028]$ $x^*_{2050} \in [355, 634]$
2016–2021	1.022	100%	$x^*_{2082} \in [1158, 2071]$ $x^*_{2050} \in [577, 1032]$

Notes: The value $x_k \in [x_{kL}, x_{kU}]_{DFO}$ is the percentage of times that the SSB predicted by the model at the end of the k-year period, x_k, falls within the confidence interval estimated by DFO for the SSB level observed at the end of the k-year period (Table 1). The value x_k^* is the SSB level achieved in the year k.

predicted by the model for the year 2015 always falls (one hundred per cent) within the confidence interval estimated by DFO for that year (row 2, and Table 1). Ninety-six and eighty-eight percent of the times the SSB predicted by the model for the years 2016 and 2017, respectively, falls within the confidence interval estimated by DFO for those years (rows 3 and 4, and Table 1). In contrast, the model does not fit well with the growth of the SSB observed during the years 2015, 2016, and 2017, if the SSB has grown, from the year 2014, at the high rate which is consistent with the observed dynamics during the 2011–2014 period, λ_n =1.37 (Table 7, rows 5–7).

Thus, the model allows us to characterize the whole post-collapse period (2004–2016) as a period of medium-high productivity, by obtaining the high levels of productivity $\frac{C}{x_{\min}} \in [1.91,1.99]$ and $\frac{C}{x_{\min}} \in [1.94,2.01]$ which are consistent with the observed dynamics during the post-collapse periods (2004–2011), (2011–2014), and (2014–2016) (Table 6, rows 3 and 4, and Fig. 3 for the average of these levels of productivity). This result is consistent with the observed average of RPS during the whole post-collapse period (2004–2016), which was greater than that observed during the pre-collapse period (1983–1990) (Morgan, 2019).

3.2.4. The most recent period (2016–2021) and predictive power of the model

Age-specific data, as used above, are not yet available for the most recent years, as the NCS assessment in the year 2022 has been cancelled by DFO. In this regard, the CSPE cannot be obtained for the most recent period (2016–2021). However, useful information on this period can be obtained from NAFO (2021), providing estimates of the SSB and the confidence interval for the SSB estimated for the year 2021 (Table 1). These estimates show the slow growth of the SSB observed during the most recent period (2016–2021) (NAFO, 2021, Fig. xii.1.) where F_n remains very low, but the current M_i were at the higher range of the past decade. Additionally, productivity conditions in recent years are similar to those estimated for the pre-collapse period (Morgan, 2019).

Based on the above, the predictive power of the model for the most recent period (2016–2021) can be evaluated using the productivity levels $\frac{C}{x_{\min}} \in [0.85,0.96]$ and growth rates $\lambda_n \in [1,1.022]$ consistent with the observed dynamics obtained for the pre-collapse period (1983–1990). In this case, using Eq. (10) (case *i)*), the model fits well with the slow growth of the SSB observed during the most recent period (2016–2021) (Table 6, row 5). The reason for this is that, from the confidence interval estimated by DFO for the SSB level at the start of the period (for the year 2016) (Table 1), the SSB predicted by the model for the year 2021 always falls (one hundred per cent) within the confidence interval estimated by NAFO (2021) for that year (Table 1).

Thus, transient dynamics show that the levels of productivity and the low growth rates consistent with the observed dynamics during the pre-collapse period (1983–1990), are also consistent with the observed dynamics for the most recent period (2016–2021). Consequently, it is also characterized by medium-low productivity (Fig. 3). This result is consistent with the above information from Morgan (2019) and NAFO (2021). Additionally, if these levels of productivity, and the low growth rates, are kept constant since 2021, it would take a long time to reach an SSB equilibrium $\overline{x} > B_{\text{lim}}$=1133 due to the slow growth of the SSB (Table 7, rows 8 and 9, column 2), where more than 60 years are required to reach a high SSB level $x^* > B_{\text{lim}}$=1133 (Table 7, rows 8 and 9, column 4). Even the predicted stock for the year 2050, x^*_{2050}, is far from B_{lim}=1133 (Table 7, rows 8 and 9, column 4).

4. Discussion

4.1. Estimation of the stock-recruitment function (SRF) and B_{lim}

Existing methods are unable to cope with transient dynamics, with the consequent lack of a SRF to identify a clear breakpoint B_{lim}, which has recently emerged in depleted, or previously depleted and recovering stocks (e.g. DFO, 2019a, for the NCS; González-Troncoso et al., 2013; González-Costas et al., 2019, for cod stock in NAFO division 3M).

Considering the NCS, we have shown that transient dynamics allow us to analyze the case of the HS with B_{lim} having higher SSB values than observed. We have shown that a HS with B_{lim}=1133 fitted by NLS is the model of best fit. This allows us both to detect the linear relationship between SSB and recruitment and to guarantee the underlying hypothesis that the SSB was always below B_{lim}, as suggested, but not tested by DFO (2019a). ICES (2021) also suggests that, with this linear relationship, and with clear evidence that recruitment is impaired, with no clear asymptote in recruitment at high SSB, B_{lim} may be at higher SSB values than observed. We have also shown that this model is also consistent with the observed population dynamics.

We have shown that transient dynamics also allow us to analyze the case of the HS with B_{lim} being the highest observed SSB, B_{lim}=893, as suggested, but not tested by DFO (2019a). In this case, the hypothesis that the SSB was always below B_{lim} is not met. Considering the pre-collapse period (1983–1990), we have shown that this model is also consistent with the observed population dynamics, with results that would also be obtained for $B_{\text{lim}} \in [893,1133)$, and for the different periods considered in this paper. This is due to the fact that, in analyzing the CSPE, the productivity levels consistent with the observed population dynamics are very similar for values of $x_{\min} \in [893,1133]$.

Thus, transient dynamics show that a HS with $B_{\text{lim}} \in [893,1133]$ fitted by NLS is the model of best fit to data which is also consistent with the observed population dynamics for the NCS. This suggests that the true breakpoint B_{lim} of this stock has not yet been observed, as suggested, but not tested, by DFO, and by other modelling results based on knowledge of fishery history (DFO, 2019a, and references therein). Additionally, this interval includes B_{lim}=1000 suggested by Rose and Walters (2019), and is slightly higher than B_{lim}=800 suggested by DFO (2011, 2019a), which is defined as the average SSB during the 1980s.

We have also shown that many SRF show similar fits to data, already commonly observed, but also the different regression methods, with different error distribution assumptions, provide quite different estimates of B_{lim}, even for the same fitted SRF. In this regard, we have shown that the HS fitted by FLR is not consistent with the observed population dynamics for the NCS, dramatically underestimating B_{lim}.

These results show that transient dynamics are crucial in analyzing the consistency with the observed population dynamics. If transient dynamics are neglected, as with existing methods, the standard criterion of the goodness of fit to the data of a particular method used in regression analysis could not guarantee a proper estimation of the SRF. In this case, the key reference point B_{lim} could be underestimated, with the consequent potential lack of sustainability and potential collapse of the stock.

Thus, in contrast to existing methods, transient dynamics allow us to test the safety of different B_{lim} provided by different regression methods by detecting those B_{lim} which are not consistent with the observed population dynamics. In this way, the age-specific mortality model (ASMM) developed in this paper allows us to properly estimate the HS and its associated B_{lim}, based not only of the standard criterion of goodness of fit, which could be met by different regression methods, but also on the consistency with the observed population dynamics.

4.2. Sustainability of F_{MSY}

We have shown that the ASMM, in contrast to existing methods, allows us to determine a CSPE which depends on the main components of population productivity, including age-specific natural mortality rates. We have also shown that transient dynamics analysis, also in contrast to existing methods, is concerned not only with the existence or nonexistence of a positive SSB equilibrium, but also with the growth rate of the SSB and the time required to achieve it. These results show that the ASMM could be a useful tool for analyzing the sustainability of the key reference points, such as F_{MSY}, and for predicting stock recovery rates also based on the observed population dynamics. In this regard, for different relevant periods, we have determined the levels of productivity (medium-low or medium-high), and their corresponding growth rates (low or high) of the SSB, which are consistent with the observed population dynamics for the NCS.

Under the Precautionary Approach, variations in population productivity should be considered when establishing key reference points in order to take into account periods of high and low productivity (Morgan, 2019; DFO, 2019b). Additionally, age-specific natural mortality rates are an important component of productivity and could affect the estimation of key reference points (Morgan et al., 2014a). These rates have a significant influence on fisheries stock assessment and management (Maunder et al., 2023). Consequently, age-specific natural mortality rates should also be considered when analyzing the sustainability of key references points. In this regard, the ASMM could be a useful tool for providing sustainability-based reference points, such as $B_{\lim}$ and F_{MSY}, under age-specific natural mortality rates and varying levels of population productivity.

4.3. Potential collapse of the stock: implications for fisheries management

We have shown that $F_{MSY} \in [0.2, 0.297]$ was at the breakpoint $B_{\lim}$=1133 (F_{MSY} close to F_{crash}) during the pre-collapse period (1983–1990). The proximity between F_{crash} and F_{MSY}, not uncommon in the case of a HS, should be verified in each species analyzed in order to avoid the automatic application of default methods (ICES, 2011). This proximity has been found in Cod stocks (Morgan et al., 2014a), Blue Whiting, and Norwegian Spring Spawning Herring (ICES, 2010). The North Sea cod is an example of the contrary (ICES, 2011).

The fishing mortality rate of the SSB estimated by DFO for this period, F_n=0.2, was close to $F_{MSY} \approx F_{crash}$. Additionally, F_n=0.2 coincides with the fixed fishing mortality rule $F_{0.1}$=0.2 applied to the NCS during much of this period (1984–1988), where $F_{0.1}$ is a yield per recruit reference point (Shelton, 1998). This implies that precautionary considerations were not taken into account during the pre-collapse period (1983–1990). This is due to the fact that the NCS fishery was managed by considering F_{MSY} as a target to be achieved rather than a limit to be avoided given the potential for collapse, as eventually took place. This scenario of potential collapse of the stock, even for low fishing mortality rates, is not contemplated by existing methods, which neglect age-specific natural mortality rates and transient dynamics.

We have shown that if F_n= 0.2 and high M_i, as estimated by DFO for this period, had been kept constant since 1990, it would take a long time to reach SSB equilibrium due to the slow growth of the SSB. This implies that, even if $F_{0.1}$=0.2 had been kept constant since 1990, the fishery would have been managed on a knife-edge, in a state of permanent tension where the stock is always below $B_{\lim}$ and extremely vulnerable to changes in productivity. Thus, the combination of the lack of precautionary management and high M_i were unable to anticipate periods of lower productivity, as eventually was the case.

By contrast, under the standard assumption of M =0.2, we have shown that, if $F_{0.1}$=0.2 had been kept constant since 1990, SSB equilibrium at very high SSB levels, which have never been observed, is achieved in just four years. This is due to the extremely high growth of the SSB, which is also not consistent with that observed. Thus, it is not surprising that the fishing mortality control rule was doubled, F_n=0.44, in the late 1980s (Shelton, 1998). However, even in this case we have shown that a high SSB equilibrium well above $B_{\lim}$ is achieved in the short-term. This implies that the standard assumption of M =0.2 led to the misperception that a precautionary management regime was in fact being applied to the NCS and, consequently, myopic harvest control rules, as $F_{0.1}$=0.2, were perceived as sustainable in the long term by neglecting high M_i.

We have shown that an SSB equilibrium above $B_{\lim}$ could have been achieved in the short-term, even with high M_i, as estimated by DFO, if precautionary management had been carried out in the late 1980s, consisting of lower $F_n \in [0.1, 0.15]$, well below F_{MSY}. These are also sustainable under $F_{MSY} \in [0.15, 0.2]$, as obtained by Rose and Walters (2019), and F_{MSY} =0.17, as obtained by Schijns et al. (2021), and lower than those obtained by Hutchings (2009), $F \in [0.13, 0.22]$, to prevent fisheries-induced evolution. This shows that, for low age-specific fishing mortality rates (lower than F_{MSY}) and sufficiently low age-specific natural mortality rates, the CSPE and transient dynamics guarantee the sustainability of key reference points, such as F_{MSY} and, consequently, the precautionary management of fish stocks. In this regard, the ASMM provides theoretical support to existing methods which fail to account for age-specific natural mortality rates, variations in population productivity, the characterization of the equilibriums, their stability properties and transient dynamics.

It should be noted that during the period 1972–1975, the NCS was managed by $F_{\max}$, the fishing mortality giving the maximum yield (Shelton, 1998). The fixed fishing mortality control rule $F_{0.1}$=0.2, generally used as a target, became the management rule and a longer-term objective during much of the pre-collapse period (1983–1990). The reason for this is that $F_{0.1}$=0.2 was considered, in contrast to $F_{\max}$, to be a conservation measure (Shelton, 1998). Based on the above, and using current reference points such as F_{MSY}, which did not exist at that time, we have shown that the shift in management objectives from maximum yield ($F_{\max}$) to $F_{0.1}$=0.2 was not enough to prevent the collapse. In this regard, myopic harvest control rules, as $F_{0.1}$=0.2, should not be interpreted as criticism of past management decisions. The lesson to be learned from the results is that precautionary management reference points should have been implemented before the stock began to collapse.

We have shown that, during the collapse period (1991–1994), F_{MSY} was unsustainable under both the extremely high M_i estimated by DFO and the more reasonable (lower) M_i estimated by Rose and Walters (2019). This result confirms that lower productivity and a reasonable, but still high, M_i exacerbated overfishing resulting in stock collapse (Rose and Walters, 2019).

4.4. Collapse and slow recovery: implications for conservation

Using a rigorous robustness requirement, we have shown that the ASMM allows for robust short-term forecasting. For the most recent period (2016–2021), we have shown that the recovery of the NCS remains distant. This scenario of stock collapse followed by very slow recovery, despite the existence of a stable positive SSB equilibrium (F_{MSY} is sustainable) and low fishing mortality, is not contemplated in existing methods. This is because these methods are based only on the existence or nonexistence of SSB equilibrium, neglecting age-specific mortality rates, varying levels of population productivity and transient dynamics.

We have shown that, even for low fishing mortality, as estimated by DFO, very slow recovery of the stock could be expected due to low productivity and high age-specific natural mortality rates. In this case, in contrast to existing methods, no level of fishing mortality F_n is sustainable, despite the existence of a stable positive SSB equilibrium. This shows that strict compliance with a moratorium on fishing must be an essential feature of recovery plans.

The robustness of the ASMM for short-term periods is consistent with observed productivity in the short-term, as there is no evidence of long periods of low or high productivity (Morgan, 2019). Thus, using as future scenarios the growth rates obtained by the ASMM for the observed short-term periods of high and low productivity, the ASMM, in contrast to existing methods, could be an effective tool in predicting stock recovery rates under both age-specific natural mortality rates and varying levels of population productivity. Consequently, the ASMM could be useful in providing scientifically-sound management strategies and sustainability-based reference points.

This paper made use of estimates from DFO, as DFO provides the official assessment model. However, the ASMM could contribute to the ongoing discussion as to whether high age-specific natural mortality rates M_i alone were the main cause of the collapse of the NCS in the late 1980s, and the slow recovery since then, as suggested by DFO, or high fishing mortality with lower, but still high, M_i, as suggested by Rose and Walters (2019). In this regard, the ASMM is highly flexible in analyzing transient dynamics for estimates of F_i and M_i according to those different approaches. This is because cohort survival rates β_i are a key parameter in the CSPE and, consequently, any increase in F_i and/or M_i has the same effect as a decrease in β_i. In this regard, the ASMM does not provide a third opinion but rather a neutral and useful tool for analyzing the sustainability of key references points under both age-specific natural mortality rates and varying levels of population productivity.

5. Conclusions

Key precautionary approach reference points, such as B_{lim}, based only on the standard criterion of the goodness of fit to the data, and MSY reference points, such as F_{MSY}, based only on the existence of a positive SSB equilibrium, might not be enough to prevent stocks collapses. Scientific advice and existing methods, based on these reference points with constant population productivity and constant low natural mortality rates, are unable to detect potential stock collapse, and collapse followed by very slow recovery, despite the existence of a positive SSB equilibrium and low fishing mortality. Thus, existing methods are unable to guarantee the sustainability of key references points.

We have shown that transient dynamics are critical for understanding and predicting the consequences of the lack of precautionary management and the neglect of variations in population productivity and age-specific natural mortality. By considering short-term population responses to variations in population productivity and survival rates (variations in age-specific fishing and age-specific natural mortality rates), scientific advisory bodies and managers could develop more robust and precautionary harvest strategies for the sustainable management of fisheries. In this regard, our results suggest that the characterization of the equilibriums, their stability properties, transient dynamics and changes in productivity (including age-specific natural mortality rates) should play a central role for fisheries management and conservation.

5.1. Future research

The ASMM could be a useful tool for analyzing other important fisheries by also including other important reference points, such as those based on yield per recruit and spawner per recruit (Morgan et al., 2014a, 2014b), as well as those based on a precautionary approach (Froese et al., 2016).

In Maroto and Morán (2014), a total biomass model for the NCS is developed to detect depensation (declines in growth rates as the population is reduced). Morgan et al. (2016) analyze the potential impact of compensation (increases in growth rates as the population is reduced) on SSB growth rate G. The lowest potential maximum G (lowest resilience) among cod stocks was found for the NCS. In this regard, the ASMM could be a useful tool for detecting compensation or depensation in depleted fish stocks by exploring further the relationship between G and the ASMM.

The estimation of the SRF could be improved if more data were available. A new model xteNCAM was used by DFO (2019a) in order to extend the observed period to 1962. A clear breakpoint B_{lim} was not identified by DFO for the period (1962–2018) and, consequently, xteNCAM has not been accepted for use as the official assessment model (DFO, 2019a). The ASMM could provide a useful tool for equilibrium and transient dynamic analysis for this extended period, when more robust estimates from DFO become available.

Credit author statement

Diana González-Troncoso: Conceptualization, Methodology, Software, Writing- Reviewing José M. Maroto: Conceptualization, Methodology, Software, Writing- Reviewing, Writing- Original draft preparation M. Eugenia Mera: Conceptualization, Methodology, Software, Writing- Reviewing Manuel Morán: Conceptualization, Methodology, Software, Writing- Reviewing.

Declaration of competing interest

The authors declare that they have no known competing financial interests or personal relationships that could have appeared to influence the work reported in this paper.

Data availability

All data were assembled from open literature reports from DFO Can. Sci. Advis. Sec. Sci. Advis. Rep., and NAFO SCS Doc.

Acknowledgements

We acknowledge support from grant number PR3/23-30830 from Complutense University-Santander bank. We are grateful to P. Regular, G.A. Rose, and C.J. Walters for sharing data on the Northern cod stock.

References

Brattey, J., Cadigan, N., Dwyer, K.S., Healey, B.P., Ings, D.W., Lee, E.M., Maddock Parsons, D., Morgan, M.J., Regular, P., Rideout, R.M., 2018. Assessment of the northern cod (Gadus morhua) stock in NAFO divisions 2J3KL. In: 2016. DFO Can. Sci. Advis. Sec. Res. Doc. 2018/018. https://waves-vagues.dfo-mpo.gc.ca/library-bibliotheque/40702017.pdf.

Cadigan, N.G., 2006. Local influence diagnostics for quasi-likelihood and lognormal estimates of a biological reference point from some fish stock and recruitment models. Biometrics 62, 713–720. https://doi.org/10.1111/j.1541-0420.2005.00517.x.

Cadigan, N.G., 2016. A state-space stock assessment model for northern cod, including under- reported catches and variable natural mortality rates. Can. J. Fish. Aquat. Sci. 73 (2), 296–308. https://doi.org/10.1139/cjfas-2015-0047.

DFO, 2011. In: Proceedings of the Newfoundland and Labrador Regional Atlantic Cod Framework Meeting: Reference Points and Projection Methods for Newfoundland cod Stocks; November 22-26, 2010. DFO Can. Sci. Advis. Sec. Proc. Ser. 2010/053. https://www.dfo-mpo.gc.ca/csas-sccs/Publications/Pro-Cr/2010/2010_053-eng.html.

DFO, 2018. Stock assessment of northern cod (NAFO divisions 2J3KL) in 2018. DFO Can. Sci. Advis. Sec. Sci. Advis. Rep. 2018/038. https://waves-vagues.dfo-mpo.gc.ca/library-bibliotheque/4071407x.pdf.

DFO, 2019a. Evaluation of the biomass limit reference point for northern cod (NAFO divisions 2J3KL). DFO Can. Sci. Advis. Sec. Sci. Advis. Rep. 2019/058 https://waves-vagues.dfo-mpo.gc.ca/library-bibliotheque/40872701.pdf.

DFO, 2019b. Stock assessment of northern cod (NAFO division 2J3KL) in 2019. DFO Can. Sci. Advis. Sec. Sci. Advis. Rep. 2019/050 https://waves-vagues.dfo-mpo.gc.ca/library-bibliotheque/40872142.pdf.

Duplisea, D.E., 2012. Equilibrium estimates of F_{msy} and B_{msy} for 3Pn4RS cod. DFO Can. Sci. Advis. Sec. Res. Doc. 2012/171 https://waves-vagues.dfo-mpo.gc.ca/library-bibliotheque/348698.pdf.

Froese, R., Coro, G., Kleisner, K., Demirel, N., 2016. Revisiting safe biological limits in Fisheries. Fish Fish. 17, 193–209. https://doi.org/10.1111/faf.12102.

González-Costas, F., González-Troncoso, D., Fernández, C., Urtizberea, A., Alpoim, R., Avila de Melo, A., De Oliveira, J., Apostolaki, P., Brunel, T., García, D., 2019. Potential operating models, harvest control rules and performance statistics for the NAFO 3M cod MSE. NAFO SCR Doc.19/001. Serial No. N6903. https://www.nafo.int/Portals/0/PDFs/sc/2019/scr19-001.pdf.

González-Troncoso, D., Morgan, J., González-Costas, F., 2013. Biological reference points of 3M cod. In: NAFO SCR Doc, 13/50. Serial No. N6207. https://www.nafo.int/Portals/0/PDFs/sc/2013/scr13-050.pdf.

Hutchings, J.A., 2009. Avoidance of fisheries-induced evolution: management implications for catch selectivity and limit reference points. Evol. Appl. 2 (3), 324–334. https://doi.org/10.1111/j.1752-4571.2009.00085.x.

ICES, 2010. Report of the Working Group on Widely Distributed Stocks (WGWIDE), 28. August – 3 September 2010, Vigo, Spain. ICES CM 2010/ACOM:15. https://doi.org/10.17895/ices.pub.19268621.v1.

ICES, 2011. Report of the workshop on implementing the ICES Fmsy framework (WKFRAME-2). ICES CM 2011/ACOM: 33. https://doi.org/10.17895/ices.pub.19280882.v1.

ICES, 2014. Report of the Workshop to consider reference points for all stocks (WKMSYREF2). ICES CM 2014/ACOM: 47. https://doi.org/10.17895/ices.pub.19283177.v1.

ICES, 2021. ICES fisheries management reference points for category 1 and 2 stocks; Technical Guidelines. In: Report of the ICES Advisory Committee, 2021. ICES Advice. https://doi.org/10.17895/ices.advice.7891, 2021, Section 16.4.3.1.

Julious, S.A., 2001. Inference and estimation in a changepoint regression problem. J. R. Stat. Soc. - Ser. D Statistician 50, 51–61. https://doi.org/10.1111/1467-9884.00260.

Kell, L.T., Mosqueira, I., Grosjean, P., Fromentin, J.-M., Garcia, D., Hillary, R., Jardim, E., Mardle, S., Pastoors, M.A., Poos, J.J., Scott, F., Scott, R.D., 2007. FLR: an open-source framework for the evaluation and development of management strategies. ICES J. Mar. Sci. 64, 640–646. https://doi.org/10.1093/icesjms/fsm012.

Maroto, J.M., Morán, M., 2014. Detecting the presence of depensation in collapsed fisheries: the case of the Northern cod stock. Ecol. Econ. 97, 101–109. https://doi.org/10.1016/j.ecolecon.2013.11.006.

Maroto, J.M., Morán, M., 2019. Transient dynamics: equilibrium, collapse, and extinction in age-structured models. The case of the Northern cod stock. Ecol. Model. 398 (24), 35–43. https://doi.org/10.1016/j.ecolmodel.2019.02.006.

Maunder, M.N., Hamel, O.S., Lee, H.-H., Piner, K.R., Cope, J.M., Punt, A.E., Ianelli, J.N., Castillo-Jordán, C., Kapur, M.S., Methot, R.D., 2023. A review of estimation methods for natural mortality and their performance in the context of fishery stock assessment. Fish. Res. 257, 106489 https://doi.org/10.1016/j.fishres.2022.106489.

Mesnil, B., Rochet, M.-J., 2010. A continuous hockey stick stock–recruit model for estimating MSY reference points. ICES J. Mar. Sci. 67 (8), 1780–1784. https://doi.org/10.1093/icesjms/fsq055.

Morgan, M.J., 2019. Changes in productivity of northern cod (*Gadus morhua*) stock in NAFO divisions 2J3KL. DFO Can. Sci. Advis. Sec. Res. Doc. 2019–2052. https://publications.gc.ca/collections/collection_2019/mpo-dfo/fs70-5/Fs70-5-2019-052-eng.pdf.

Morgan, M.J., Shelton, P.A., Rideout, R.M., 2014a. An evaluation of fishing mortality reference points under varying levels of population productivity in three Atlantic cod (Gadus morhua) stocks. ICES J. Mar. Sci. 71 (6), 1407–1416. https://doi.org/10.1093/icesjms/fsu092.

Morgan, M.J., Shelton, P.A., Rideout, R.M., 2014b. Varying components of productivity and their impact on fishing mortality reference points for Grand Bank Atlantic cod and American plaice. Fish. Res. 155, 64–73. https://doi.org/10.1016/j.fishres.2014.02.019.

Morgan, M.J., Shelton, P.A., González-Costas, F., González-Troncoso, D., 2016. Compensation potential in six depleted groundfish stocks from the Northwest Atlantic. Can. J. Fish. Aquat. Sci. 73 (2), 257–269. https://doi.org/10.1139/cjfas-2015-0056.

NAFO, 2021. Report of the scientific Council, 27 may -11 June 2021. NAFO SCS Doc.21/14REV. https://www.nafo.int/Portals/0/PDFs/rb/2021/redbook_final_web2021.pdf.

Rose, G.A., Walters, C.J., 2019. The state of Canada's iconic Northern cod. A second opinion. Fish. Res. 219, 105314 https://doi.org/10.1016/j.fishres.2019.105314.

Schijns, R., Froese, R., Hutchings, J.A., Pauly, D., 2021. Five centuries of cod catches in Eastern Canada. ICES J. Mar. Sci. 78 (8), 2675–2683. https://doi.org/10.1093/icesjms/fsab153.

Shelton, P.A., 1998. A comparison between a fixed and a variable fishing mortality control rule used to manage the cod stock off southern Labrador and the east coast of Newfoundland. Fish. Res. 37 (1–3), 275–286. https://doi.org/10.1016/S0165-7836(98)00143-X.